

CAPABILITY OF SEGMENTED ANNULAR ARRAYS TO GENERATE 3-D ULTRASONIC IMAGING

PACS REF.: 43.38.HZ, 43.35, 43.35.BC, 43.60

Ullate Luis G.; Martínez Oscar; Akhnaq Mostafa; Montero Francisco
Instituto de Automática Industrial (CSIC)
La Poveda,
Arganda del Rey, 28500, Madrid
Spain
Tel: (34) 91 871 19 00,
Fax: (34) 91 871 70 50
e-mail: luisg@jai.csic.es

ABSTRACT

The main object of this paper is to show the influence of the array geometry on the image properties. This is made by comparing the beam generated by three 2D arrays: a squared array, a regular segmented annular array with a star distribution of elements and a segmented annular array with elements of unitary aspect ratio. The three arrays are equivalent in the sense that their size, number of active elements and active areas are similar and that they emit the same ultrasonic pulse. After analysing theoretically the main beam and grating lobes in the steering case, the paper concludes advising to use segmented annular arrays with elements of unitary aspect ratio as they produce ultrasonic beams with good properties even for an inter-element spacing of 1.1λ .

INTRODUCTION

In the last years the interest on 3D ultrasonic imaging based on 2D arrays is increasing. Conventional 2D arrays are formed by square elements distributed in a matrix grid. This distribution has high periodicity level causing grating lobes of high intensity, which limit the image contrast. In order to reduce grating lobes the inter-element spacing is reduced to half a wavelength [1], but from this condition three obstacles arise [2]: (a) The thousands of transducer elements demand constructing such a number of channels that overpass the capability of the present technology, (b) connections are difficult to fabricate and (c) the small size of elements is associated to low signal to noise ratios (SNR).

Some of these problems have been investigated, and in fact, different thinning strategies have been developed to reduce the number of active elements, maintaining, at the same time, good field characteristics [3-6]. SNR for such solutions can however become low in excess.

As an alternative to squared arrays, segmented annular (SA) arrays have been proposed [7]. SA arrays have two advantages compared to squared arrays (Figure 1). First, their axial symmetry provides regularity in the field radiated and, second, their geometry entails a reduction of the periodicity level and therefore of the intensity of the grating lobes. This fact allows applying inter-element spacing higher than $\lambda/2$ in the array and, at the same time, increasing the element size and reducing the number of resources needed. The aspects associated to the computation and theoretical analysis of the ultrasonic field generated by SA arrays can be found in references [7-9].

The image properties depend on several factors like the array geometry, the waveform of the ultrasonic pulse, the focussing delays in emission and reception and apodization functions,

among others. All these parameters can be modified in order to improve a given experiment, but it is the transducer who mainly causes limitations on the quality of ultrasonic imaging. The main object of this paper is to show the influence of the array geometry on the image properties. This is made by comparing the beam generated by three 2D arrays: a squared array (SQ), a regular SA array (R-SA) with a star distribution of elements and a SA array with elements of unitary aspect ratio (U-SA) (Figure 1). The three arrays are equivalent in the sense that their size, number of active elements and active areas (around 70%) are similar and that they emit the same ultrasonic pulse. The image properties are analysed on the basis of the following example: the three arrays have a diameter of 15λ . SQ has 124 squared elements with inter-element distance of 1.1λ and square size of λ . The R-SQ array has 25 elements in each one of its 5 rings, which are 1.1λ interspaced. The U-SA array also has 128 elements with inter-element spacing of 1.1λ , which are distributed in four rings. The case of beam steering focusing at ($r^F=28\text{mm}$, $\theta^F=30^\circ$, $\phi^F=0^\circ$) is considered in simulations.

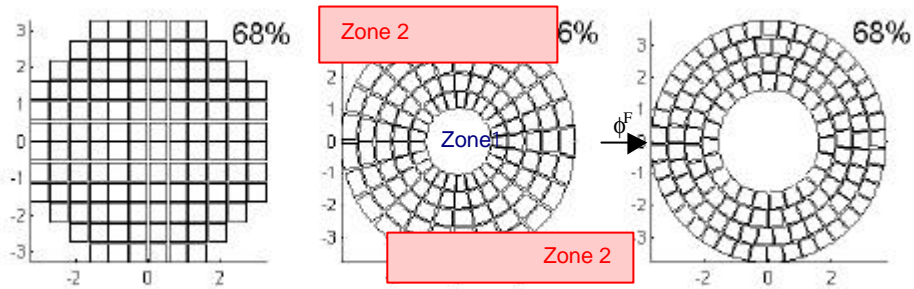


Figure 1: SQ array, R-SQ array and U-SQ array

Figure 2 shows for the three arrays a C-class representation of the emission-reception beam at the focal plane, in the case of 30° steering. Some differences on the beam properties can be observed in the figure that will be discussed with more detail in the following sections, where the main beam and grating lobes are analysed separately.

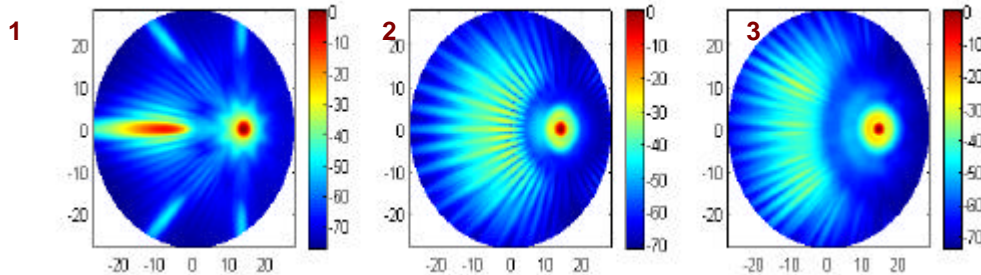


Figure 2: C-class representation of the projection over the transducer plane of the focal semi-sphere with radius equal to the focal distance (28mm). (1) SQ array, (2) R-SQ array and (3) U-SQ array. In the axis is shown the distance in mm.

MAIN BEAM PROPERTIES

In the normal radiation case, the three arrays produce main beams of very similar properties for the three arrays considered. The beam has a circular shape and its width coincides with spherically focused transducers [10]:

$$\Delta q = 2K_a \arcsin \frac{l}{D} \quad (1)$$

where K_α is a coefficient that is given in Table 1 for the different cutting levels in pulse-echo, for in continuous wave (CW):

| TABLE 1 | -6dB | -12dB | -24dB | -36dB |
|-----------------|------|-------|-------|-------|
| K_α (CW) | 0.51 | 0.70 | 0.93 | 1.05 |

With wide band ultrasonic pulses, the main lobe is slightly narrower than those shown in the table.

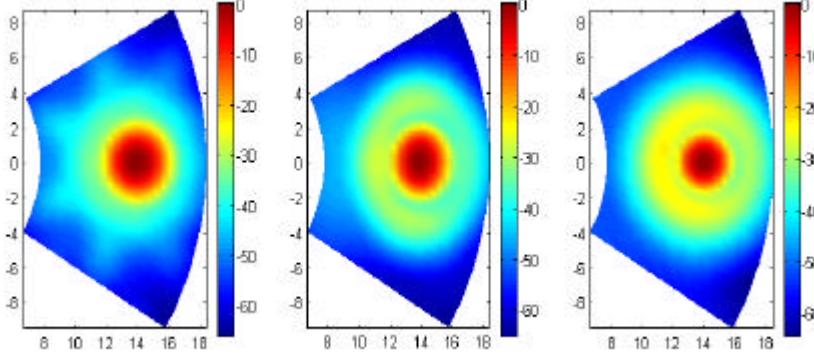


Figure 3. Detail of the main beam (1) SQ array, (2) R-SA array and (3) U-SA array

In figure 3 a detail of the steered main beam for the three apertures. The value of K_α (dB) for different amplitude levels is shown in table II. The main beam of SQ is circular, and it is wider than the one produced by the rest of apertures because it is not perfectly adjusted to the external circumference of the transducer. However, the main beam becomes the narrowest in its lower part. The main beam of the R-SA aperture has an oval section. An explanation of this effect is given with the help of figure 1(c), where the aperture has been divided in two zones. The elements of Zone 1 present a wide lateral response in the focal azimuth direction ϕ^F and, therefore, contribute largely to the main beam formation. However, the elements of Zone 2 have a narrow lateral response in the focal direction ϕ^F and, therefore, their contribution to the field is reduced. It can be said that when the element aspect ratio is far from unity, with one of the dimensions much larger than a wavelength, the SA array tends to behave like a linear array instead of a 2D array. The main beam of the U-SA aperture is the narrowest for amplitudes above -25dB, however, it widens in its lower part due to the secondary lobes produced by the central hole of the array.

| TABLE 2 | -6dB | -12dB | -24dB | -36dB |
|-------------------|------|-------|-------|-------|
| K_α (SQ) | 0.71 | 0.95 | 1.31 | 2.14 |
| K_α (R-SA) | 0.63 | 0.84 | 1.15 | 2.46 |
| K_α (U-SA) | 0.59 | 0.78 | 1.1 | 2.6 |

An additional parameter useful for estimating the capability of 2D arrays is the array lateral response $K_d(\theta^F)$. This parameter indicates the loose of intensity at the focal point, as a function of the steering angle. In the case of a squared array and CW conditions in one way, this function is determined by the elements' lateral response:

$$K_d = \sin c\left(\frac{e}{l} \sin(\mathbf{q}^F)\right) \quad (2)$$

where e is the element side dimension.

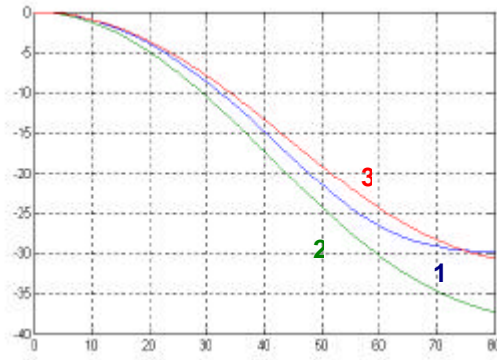


Figure 4. Amplitude at the focus in pulse-echo varying the steering angle from 0° to 80° , (1) SQ, (2) R-SA and (3) U-SA

This function modulates the main beam, and it has zeros in the space of interest when the elements size is greater than 1.2λ . In the case of the U-SA aperture, it can be shown [9] that the lateral response is approximately determined by the element lateral response. When the elements are very small, their geometry is close to a square and, in this case, K_d in CW conditions is also given by Equation (2). In contrast, as R-SA has elements with aspect ratio far from unity, its lateral response is lower than the other two arrays. The elements' size diversity proper of star arrays (R-SA), however, prevents the existence of zeros in its lateral response. Figure 4 shows the lateral response of the three arrays; SQ and U-SA have very similar lateral responses with a drop in amplitude below -15dB steering angles below 45° .

GRATING LOBES FORMATION

The existence of grating lobes is a very important limitation in ultrasonic imaging based on 2-D phased arrays. Due to the inter-element periodicity, lobes of high amplitude can be formed in certain directions where the time interval between element impulse responses equals one period of the ultrasonic signal. In this section, grating lobes from the three considered arrays are presented and analysed.

A 2-D squared array produces grating lobes at its main directions where they have a maximum periodicity level. Grating lobes are deviated from the focusing elevation by an angle \mathbf{q}_{GL} :

$$\mathbf{q}_{GL} \approx -\arcsin(\mathbf{l}/d - \sin \mathbf{q}^F) \quad (3)$$

where d is the inter-element spacing. This expression indicates that for larger d , the distance between the main lobe and grating lobes is shorter. The grating lobes amplitude A_{GL} in CW conditions is also well known [11]:

$$A_{GL} = \sin c\left(\frac{e}{\mathbf{l}} \sin(\mathbf{q}_{GL})\right) \quad (4)$$

where e is the element side. The image contrast is limited by the difference of amplitude between the main beam (given by eq. 2) and the grating lobes, both being modulated by the element's radiation pattern. An index of the image contrast is then given by the ratio between A_{GL} and the main lobe amplitude:

$$GL \approx \frac{\sin c(e/\mathbf{l} \cdot \sin \mathbf{q}_{GL})}{\sin c(e/\mathbf{l} \cdot \sin \mathbf{q}^F)} \quad (5)$$

In wideband conditions, the number of cycles (n_c) of the ultrasonic pulse delimits GL [11]:

$$GL \approx \frac{1}{BN^{1/2}} \frac{\sin c(d/\mathbf{l} \cdot \sin \mathbf{q}_{GL})}{\sin c(d/\mathbf{l} \cdot \sin \mathbf{q}^F)} \quad (6)$$

where B is the relative bandwidth of the ultrasonic pulse, which in the case of a rectangular envelope can be approximated to $1/n_c$ and N is the number of elements of the SQ array.

Segmented ring arrays also have certain regularities that facilitate the formation of grating lobes, although they have lower periodicity than 2-D squared arrays. Such regularities exist for any direction of the steered beam and are mainly due to two factors: first, a radial periodicity given by the distance 'e' between rings and, second, a tangential periodicity given by the inter-element spacing 'w' in each annulus. In the U-SA case, w is common for all annuli and e=w, so grating lobes spread at all azimuth directions in a ring centred on the main lobe and separated by an elevation angle θ_{GL} that is approximately given by Equation 3. Grating lobes amplitude can be theoretically estimated by introducing the concept of periodicity degree (PD) in Equation 4:

$$A_{GL} = PD \cdot \frac{B}{N^{1/2}} \sin c\left(\frac{e}{\mathbf{I}} \sin(\mathbf{q}_{GL})\right) \quad (7)$$

And the contrast index GL is in this case:

$$GL_{CW} \approx PD \frac{B \cdot \sin c(e/\mathbf{I} \cdot \sin \mathbf{q}_{GL})}{N^{1/2} \sin c(e/\mathbf{I} \cdot \sin \mathbf{q}^F)} \quad (8)$$

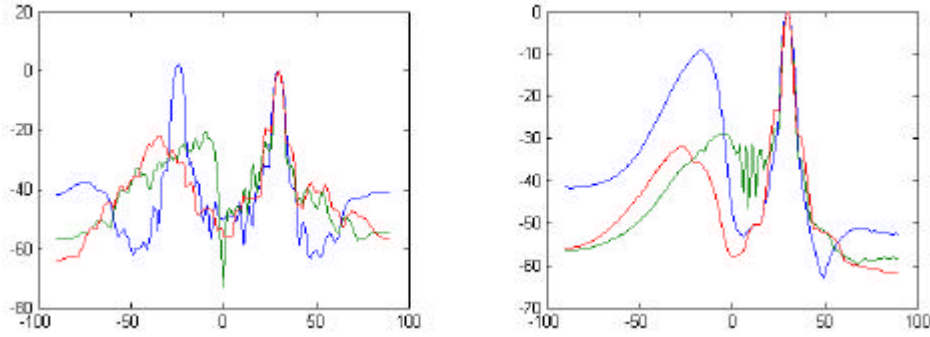


Figure 5. Elevation profiles of pressure amplitude with $\mathbf{q}^F=30^\circ$ (the maximum value for all azimuth directions has been taken) for CW (left) and wide band (right) conditions. (1) SQ array , (2) R-SA array and (3) U-SA array

The periodicity degree (PD) of an SA array can be estimated by calculating the ratio GL between the grating lobe and the main beam amplitudes, considering the array formed by ideal CW vibrating points [9]. We have made simulations for determining PD under this criterion obtaining a value of PD=0.28, which is in contrast to PD=1 proper to the main directions on SQ. The cases of SQ and U-SA arrays can be compared in wideband conditions, with the aid of the C-class representation of figure 1 and the elevation profiles of figure 5. While the grating lobes of SQ are concentrated in a small region, in the U-SA case they spread over a wider region losing much of their amplitude. Figure 4 shows that U-SA arrays reach elevation angles up to 30° with contrast level better than -32dB, although they have 1.1λ of inter-element spacing.

With respect to grating lobes formation, regular arrays with star-like configuration have a similar behaviour as other SA arrays. But they also have some particular differences. On the one hand, as w is not common for every ring, there is major diversity on the tangential periodicity causing grating lobes to extent through a larger area. On the other hand, the outer rings (Zone 2 of Figure 1) have larger inter-element spacing and produce grating lobes very close to the main lobe, which at the same time are higher than in the U-SA case, due to the modulating effect of its large elements.

CONCLUSIONS

The capability of segmented annular arrays to generate volumetric imaging has been discussed for the case of small apertures ($D \leq 20\lambda$). The image properties have been analysed on the basis of three 2D arrays of equivalent geometry (circular with $D=15\lambda$), full active area and same number of elements ($N \approx 128$). SQ is a 2D array of squared elements, U-SA is a segmented annular array with elements of unitary aspect ratio, and R-SA is a segmented annular array with

star-like configuration. On the one hand, the main beam properties (regularity, lateral resolution and variation of the focal amplitude with respect to the elevation angle) have been analysed concluding that while SQ and U-SA have similar good results, R-SA suffers a deterioration advising against using this type of arrays as phased arrays. On the other hand, the grating lobes have also been analysed. Several expressions have been shown which allow an approximate prediction of the grating lobes generated by segmented annular arrays (p.e. position, amplitude, etc). As the inter-element distance of SQ is close to a wavelength, this array produces grating lobes of high amplitude which prevent this array to be used as phased array. Segmented annular arrays have lower periodicity level than squared arrays, causing grating lobes of lower amplitude. In particular, U-SA produces grating lobes which are ??dB (CW) and ?? dB (wide band) below the ones of SQ. Segmented annular arrays with star-like configuration have however grating lobes of higher intensity than U-SA.

Acknowledgements:

The authors thank to the CAM and CE for the postdoctoral grant to Oscar Martínez. The supports from CICYT DPI2001-2156-C02-02 and DPI-2001-2043 projects are also acknowledged.

REFERENCES

- [1] Light, E.D., Davidsen, R.E., Fiering, J.O., Hruschka, T.A., Progress in Two-Dimensional Arrays for Real-Time Volumetric Imaging, *Ultrasonic Imaging*, 20:1-15, 1998.
- [2] S.W. Smith, R.E. Davidsen, Ch.D. Emary, R.L. Goldberg and E.D. Light, "Update on 2-D array transducers for medical ultrasound", *1995 Ultrasonics Symposium*, pp. 1273-1278, 1995
- [3] Turnbull, D.H., Foster, F.S., Beam Steering with Pulsed Two-Dimensional Transducer Arrays, *IEEE Transactions on Ultrasonics, Ferroelectrics and Frequency Control*, 38:320-333, 1991
- [4] Davidsen, R.E., Jensen, J.A., Smith, S.W., Two-dimensional Random Arrays For Real Time Volumetric Imaging, *Ultrasonic Imaging*, 16:143-163, 1994.
- [5] Brunke, S.S., Lockwood, G.R., Broad-Bandwidth Radiation Patterns of Sparse Two-Dimensional Vernier Arrays, *IEEE Transactions on Ultrasonics, Ferroelectrics and Frequency Control*, 44:1101-1109, 1997
- [6] Lockwood, G.R., Foster, F.S., Optimizing the Radiation Pattern of Sparse Periodic Two Dimensional Arrays, *IEEE Transactions on Ultrasonics, Ferroelectrics and Frequency Control*, 43:15-19, 1997
- [7] Oscar Martínez Graullera: "Arrays de anillos segmentados para la generación de imagen ultrasónica", Tesis Doctoral ETSI Telecomunicaciones, (Sep. 2000).
- [8] O. Martinez, Luis G. Ullate, Francisco Montero, "Computation of the ultrasonic field radiated by segmented-annular arrays", *Journal of Computational Acoustics*, (admitida su publicación)
- [9] Luis G. Ullate, O. Martínez, A. Ibáñez, M.T. Sánchez, "Analysis of the ultrasonic field radiated by segmented annular arrays", *IEEE Trans on Ultrason. Ferroelec. And Freq. Control*, (to be accepted)
- [10] G.S. Kino, "Acoustic waves: devices, imaging, and analog signal processing", Prentice Hold Inc., 1987
- [11] A. Macovski, "Theory in imaging with arrays", *Acoustical Imaging*, Ed. G. Wade, Plenum Press, New York, 1976, pp. 111-126